Magn Reson Med Sci 2020; 19; 135–140
doi:10.2463/mrms.mp.2018-0077
Published Online: May 31, 2019

MAJOR PAPER

Quantitative Susceptibility Mapping for Carotid Atherosclerotic Plaques: A Pilot Study

Yohei Ikebe[1], Hideki Ishimaru[1*], Hiroshi Imai[2], Kuniko Abe[3], Tsuyoshi Izumo[4], Yoichi Morofuji[4], Reiko Ideguchi[1], Minoru Morikawa[1], and Masataka Uetani[1]

Purpose: Identifying plaque components such as intraplaque hemorrhage, lipid rich necrosis, and calcification is important to evaluate vulnerability of carotid atherosclerotic plaque; however, conventional vessel wall MR imaging may fail to discriminate plaque components. We aimed to evaluate the components of plaques using quantitative susceptibility mapping (QSM), a newly developed post-processing technique to provide voxel-based quantitative susceptibilities.

Methods: Seven patients scheduled for carotid endarterectomy were enrolled. Magnitude and phase images of five-echo 3D fast low angle shot (FLASH) were obtained using a 3T MRI, and QSM was calculated from the phase images. Conventional carotid vessel wall images (black-blood T_1-weighted images [T_1WI], T_2-weighted images [T_2WI], proton-density weighted images [PDWI], and time-of-flight images [TOF]) were also obtained. Pathological findings including intraplaque hemorrhage, calcification, and lipid rich necrosis at the thickest plaque section were correlated with relative susceptibility values with respect to the sternocleidomastoid muscle on QSM. On conventional vessel wall images, the contrast–noise ratio (CNR) between the three components and sternocleidomastoid muscle was measured respectively. Wilcoxon signed-rank test analyses were performed to assess the relative susceptibility values and CNR.

Results: Pathologically, lipid rich necrosis was proved in all of seven cases, and intraplaque hemorrhage in five of seven cases. Mean relative susceptibility value of hemorrhage was higher than lipid rich necrosis unexceptionally ($P = 0.0313$). There were no significant differences between CNR of hemorrhage and lipid rich necrosis on all sequences. In all six cases with plaque calcification, susceptibility value of calcification was significantly lower than lipid rich necrosis unexceptionally ($P = 0.0156$). There were significant differences between CNRs of lipid rich necrosis and calcification on T_1WI, PDWI, TOF ($P < 0.05$).

Conclusion: QSM of carotid plaque would provide a novel quantitative MRI contrast that enables reliable differentiation among intraplaque hemorrhage, lipid rich necrosis, and calcification, and be useful to identify vulnerable plaques.

Keywords: *magnetic resonance imaging, plaque imaging, intraplaque hemorrhage, quantitative susceptibility mapping*

Introduction

About 15% of strokes are thought to be caused by carotid artery atherosclerosis.[1] There has been a lot of interest in the evaluation of carotid plaque characteristics with various imaging techniques and biochemical markers.[2–4]

Based on early histopathologic studies, intraplaque hemorrhage is more highly associated with ischemic events than

[1]Department of Radiological Sciences, Nagasaki University Graduate School of Biomedical Sciences, 1-7-1 Sakamoto, Nagasaki, Nagasaki 852-8501, Japan

Received: July 27, 2018 | Accepted: April 12, 2019

[2]Siemens Healthcare K.K., Tokyo, Japan
[3]Department of Pathology, Nagasaki University Graduate School of Biomedical Sciences, Nagasaki, Japan
[4]Department of Neurosurgery, Nagasaki University Graduate School of Biomedical Sciences, Nagasaki, Japan
[*]Corresponding author, Phone: +81-95-849-7354, Fax: +81-95-849-7357, E-mail: ishi_maru@yahoo.co.jp

any other plaque components including ulceration, calcification, and lipid rich necrosis.[5,6] Another study has shown that increased stroke risk is related to plaque thrombus, macrophage infiltration, high microvessel density.[7] Several plaque imaging studies have shown that development of intraplaque hemorrhage is associated with carotid plaque progression, and it is also associated with risk factors for future ipsilateral stroke events.[8–10] Carotid vessel wall imaging is useful for tissue characterization of carotid atherosclerotic plaques. Intraplaque hemorrhage exhibits high signal intensity on T_1-weighted images (T_1WI)[11–14]; however, T_1W images were hampered by false positives from T_1W hyperintense lipid rich necrosis.[15] There are limitations on the detection of slight hemorrhage/thrombus and the discrimination of hemorrhage and lipid rich necrosis.

Quantitative susceptibility mapping (QSM) is a recently developed MRI technique that provides a quantitative measure of tissue magnetic susceptibility using gradient echo phase data. The QSM values depend on the concentration of paramagnetic species, which have positive susceptibility values, and diamagnetic species, which have negative susceptibility values. Whereas conventional susceptibility weighted images qualitatively show hypointensity for both paramagnetic and diamagnetic species, QSM can be used to differentiate paramagnetic materials (such as iron derived from hemoglobin), which have positive values, and diamagnetic materials (such as calcium), which have negative values.[16–18] Although there are few reports on the QSM of carotid atherosclerotic plaques, QSM might detect slight hemorrhage sensitively and differentiate various components of the plaque. We aimed to evaluate the components of carotid atherosclerotic plaques using QSM.

Materials and Methods

The study was conducted with the approval of our Institutional Review Board. Seven patients scheduled for carotid endarterectomy were enrolled. All patients were male, and the median age was 70 years (range 39–82). Five patients of them had cerebral infarction due to carotid atherosclerotic plaques. One patient suffered from transient ischemic attack due to carotid atherosclerotic plaque. The other patient was nonsymptomatic, and carotid atherosclerotic plaques were incidentally found. All patients underwent MRI examination on a 3T MR system (Skyra, Siemens, Erlangen, Germany) with a 20-channel head and neck coil (Siemens Healthcare, Erlangen, Germany). Multi-echo 3D fast low angle shot (FLASH) was performed using the following parameters: number of TEs, 5; first TE, 4.38 ms; TE spacing, 2.26 ms; TR, 25 ms; flip angle, 11°; FOV, 15 × 15 cm^2; acquisition matrices, 160 × 160; section thickness, 0.45 mm; imaging time, 2 min 31 s. QSM was calculated from the phase images of 3D gradient echo data using STI Suite version 2.2. (https://people.eecs.berkeley.edu/~chunlei.liu/software.html). Mask images were generated from magnitude images by threshold for background phase removal. QSM with harmonic phase removal using the Laplacian operator (HARPERELLA) was then calculated from each local tissue phase by solving an inverse problem using the iLSQR method. Conventional carotid vessel wall images were also acquired in the same examination using multicontrast sequences. The imaging parameters for T_1WI/T_2-weighted images (T_2WI), and proton-density weighted images (PDWI) were as follows: black-blood (presaturation pulse technique) two-dimensional fast-spin echo, TR/TE, 500/9.8, 4000/78, and 3000/11 ms, respectively; flip angle, 123°, 160°, and 150°, respectively; FOV, 16 × 16 cm^2; acquisition matrices, 256 × 256; section thickness, 3 mm, with a fat suppression technique. For the time-of-flight (TOF) images, the following imaging parameters were used; three-dimensional gradient echo, TR/TE, 26/2.46 ms; flip angle, 15°; FOV, 16 × 16 cm^2; acquisition matrices, 256 × 256; section thickness, 1 mm. All images were obtained in the axial plane. All patients underwent carotid endarterectomy within 40 days (range 7–39 days) from MRI, and the endarterectomy specimens were resected *en bloc*, fixed in buffered formalin, examined macroscopically, and sectioned serially at 5-mm intervals. Paraffin sections (5 μm thick) were stained with hematoxylin–eosin. The thickest plaque section, which was the narrowest portion of internal carotid artery, was selected for imaging pathologic correlation and examined for the following three components: hemorrhage, calcification, and lipid rich necrosis. Areas containing red blood cells were classified as hemorrhage. Areas containing amorphous material and cholesterol crystals were classified as lipid rich necrosis. The exact level of the selected sections was defined by reference to the level of the carotid bifurcation, and a corresponding image slice was selected. On conventional vessel wall images, the contrast–noise ratio (CNR) between the three components and sternocleidomastoid muscle was measured respectively, and we correlated CNR on each sequence and investigated the ability to identify each component. Susceptibility values of intraplaque hemorrhage, calcification, and lipid rich necrosis were measured on QSM using the ImageJ 1.49 (National Institutes of Health [NIH], Bethesda, MD, USA). QSM does not generate an absolute susceptibility because no information is available at $k = 0$ but rather a relative susceptibility between tissues. The sternocleidomastoid muscle was used as reference region for each component in our study. ROI corresponding with histopathologic findings were manually drawn by consensus with two neuroradiologists (Y.I. and H.I.). ROIs of QSM and conventional images were placed with reference to pathological findings. Wilcoxon signed-rank test analyses were performed to assess the differences among these three components.

Results

Image acquisition and post processing generating QSM succeeded in all seven cases. Intraplaque hemorrhage was proved pathologically in five of seven cases. In these five cases, the area of intraplaque hemorrhage showed markedly

Table 1 The relative susceptibility values between each component (hemorrhage, lipid rich necrosis and calcification) and sternocleidomastoid muscle

Case no.	Age (years)	Sex	History of infarction	Mean relative susceptibility values		
				Hemorrhage	Lipid rich necrosis	Calcification
1	66	Male	+	632	343	−709
2	68	Male	+	699	127	−623
3	82	Male	+	None	14	−735
4	76	Male	−	146	−125	−802
5	39	Male	+	203	56	None
6	80	Male	−	None	−50	−357
7	70	Male	+	321	21	−401

Mean relative susceptibility value of hemorrhage was higher than lipid rich necrosis in all five cases, and mean relative susceptibility value of calcification was lower than lipid rich necrosis in all six cases. Statistical analysis proved that the mean relative susceptibility values of hemorrhage were significantly higher than the values of lipid rich necrosis ($P = 0.0313$, Wilcoxon signed-rank test, $n = 5$), and the values of calcification were statistically significantly lower than the values of lipid rich necrosis ($P = 0.0156$, Wilcoxon signed-rank test, $n = 6$).

Table 2 The CNRs between each component (hemorrhage, lipid rich necrosis and calcification) and sternocleidomastoid muscle on conventional vessel wall imaging

		Contrast–noise ratios			
		T_1WI	T_2WI	PDWI	TOF
Case 1	Hemorrhage	115.3	8.7	18.3	38.7
	Lipid rich necrosis	−15.2	19	11.7	27.7
	Calcification	4.7	0.7	−1	0.3
Case 2	Hemorrhage	16.3	8.8	−3.1	20
	Lipid rich necrosis	−17.5	24.8	4.2	9
	Calcification	2	25.8	5.4	9.5
Case 3	Lipid rich necrosis	−2	8.5	4	19.2
	Calcification	20.8	16.3	−10.3	1.6
Case 4	Hemorrhage	−5.2	14.6	−6.9	−6.7
	Lipid rich necrosis	−16.3	28	7.6	4
	Calcification	−8.7	1	−6.4	−8
Case 5	Hemorrhage	13.8	93.7	14.3	46.3
	Lipid rich necrosis	−28.6	66.7	14.8	17.7
Case 6	Lipid rich necrosis	−4.3	9	9.6	37
	Calcification	2	7.8	1	26.7
Case 7	Hemorrhage	14.2	16.5	−3.4	−2.5
	Lipid rich necrosis	−18.6	30.5	−0.6	1.5
	Calcification	−9.8	3.8	−4.4	−20

There were no significant differences between CNRs of hemorrhage and lipid rich necrosis on all conventional vessel wall images (T_1WI; $P = 0.2188$, T_2WI; $P = 0.3125$, PDWI; $P = 0.1563$, TOF; $P = 0.125$, Wilcoxon signed-rank test, $n = 5$). There were significant differences between CNRs of lipid rich necrosis and calcification on T_1WI, PDWI, TOF. Although there was no significant difference on T_2WI, calcification could be identified on conventional vessel wall images (T_1WI; $P = 0.0156$, T_2WI; $P = 0.1094$, PDWI; $P = 0.0313$, TOF; $P = 0.0313$, Wilcoxon signed-rank test, $n = 5$). CNR, contrast-to-noise ratio; T_1WI, T_1-weighted image; T_2WI, T_2-weighted image; PDWI, proton-density weighted images; TOF, time-of-flight.

high relative susceptibility values on QSM (Table 1). Lipid rich necrosis was pathologically proved in all of seven cases, and the corresponding areas exhibited various relative susceptibility values. Intraplaque hemorrhage showed unexceptionally higher relative susceptibility values than lipid rich necrosis component in all five cases. Statistical analysis proved that the values of hemorrhage were significantly higher than lipid rich necrosis ($P = 0.0313$, $n = 5$). There were no significant differences between CNRs of hemorrhage and lipid rich necrosis on all conventional vessel wall images (Table 2).

Calcification was pathologically proved in six of seven cases. Areas corresponding to calcification showed markedly low relative susceptibility values on QSM in these six cases (Table 1). In all six cases, calcification showed significantly lower relative susceptibility values than lipid rich necrosis component on QSM in all six cases ($P = 0.0156$, $n = 6$). There were significant differences between CNRs of lipid rich necrosis and calcification on T_1WI, PDWI, TOF (Table 2, T_1WI; $P = 0.0156$, PDWI; $P = 0.0313$, TOF; $P = 0.0313$, $n = 6$). On T_2WI, there was no significant difference ($P = 0.1094$, $n = 6$). An example was shown in Fig. 1.

Discussion

In this study, the area corresponding to intraplaque hemorrhage showed markedly high relative susceptibility values on QSM in all five cases as expected. Normal vessel walls and calcification are diamagnetic, whereas intraplaque hemorrhage is paramagnetic.[19] This leads to opposite phase polarities, which could be utilized in QSM for better differentiation of diamagnetic components from intraplaque hemorrhage.[20] The correlations reported in this study between intraplaque hemorrhages and high relative susceptibility values would facilitate QSM-based identification of intraplaque

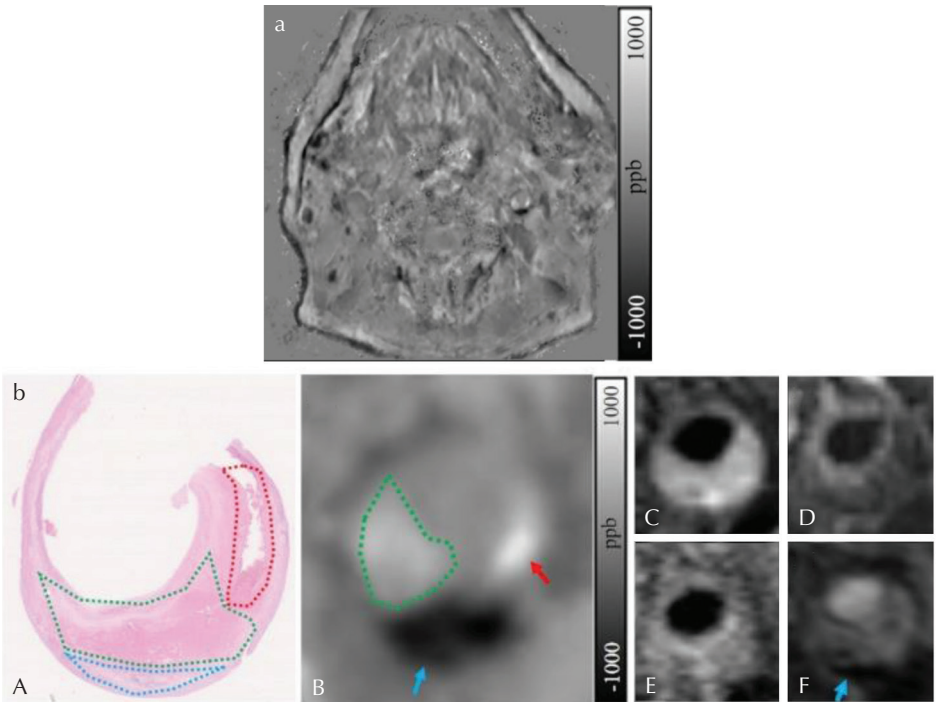

Fig. 1 (**a** and **b**) A case example (case 1). (**a**) Quantitative susceptibility mapping (QSM) image. (**b**) Focus on left carotid plaque. (**A**) Hematoxylin–eosin-stained histopathological cross-section (Hemorrhage, lipid rich necrosis, and calcification are surrounded by red, green, and blue dot lines, respectively.). (**B**) QSM, (**C**) T_1-weighted image (T_1WI), (**D**) T_2-weighted image (T_2WI), (**E**) proton-density weighted images (PDWI), (**F**) time-of-flight (TOF). Hemorrhage (red arrow) and lipid rich necrosis component (surrounded by green dot lines) were clearly differentiated on QSM (**B**), whereas on black-blood T_1WI and TOF (**C** and **F**) intraplaque hemorrhage and lipid rich necrosis showed similar signals. On TOF, calcification (blue arrow) showed low signal, but the low signal of calcification is clear on QSM.

hemorrhage. The detection and quantification of tiny foci of hemorrhage in asymptomatic carotid plaque might be possible using QSM.

Lipid rich necrosis components showed various but lower relative susceptibility values than intraplaque hemorrhage. Since lipid is diamagnetic, lipid rich necrosis was expected to show low values; however, lipid rich necrosis showed slightly high values on QSM in some cases. Although lipid content in plaques would be derived from foam cells, Kolodgie et al.[21] observed that advanced atherosclerotic plaques contained erythrocyte membranes in the necrotic core, suggesting that erythrocytes may actively contribute to plaque growth. We hypothesize that necrotic core might contain some paramagnetic material derived from erythrocytes. Further immunohistological analyses of the necrotic core are necessary to solve this question.

Distinctive differentiation between hemorrhage and lipid rich necrosis was difficult on conventional vessel wall images. On the other hand, intraplaque hemorrhage was clearly distinguished from lipid rich necrosis on QSM, since the relative susceptibility values of hemorrhage were significantly higher than lipid rich necrosis. Because carotid intraplaque hemorrhage has a much stronger association with ipsilateral ischemic events than does lipid rich necrosis, differentiation between the two components is clinically important. It is reported that carotid plaque hyperintensity on magnetization prepared rapid acquisition with gradient echo (MPRAGE), a heavy 3D T_1WI technique, is associated with previous cerebral ischemic events,[22] but MPRAGE may not differentiate the two components, because T_1W images were hampered by false-positives from T_1W hyperintense lipid rich necrosis.[15]

Calcification, which is a relatively common structural feature in human carotid atherosclerosis showed markedly low relative susceptibility values in all six cases, and the relative susceptibility values of calcification was significantly lower than lipid rich necrosis. Although there was no significant difference on T_2WI, calcification could be identified on conventional vessel wall images. Although there were significant differences between CNRs of lipid rich necrosis and calcification on T_1WI, PDWI, and TOF, QSM might offer much better contrast than that of conventional images. A recent study reported a performance of susceptibility weighted imaging for the detection of calcification,[23] and QSM can also be used to detect calcification as suggested by our study. Calcified carotid atherosclerotic plaques are less prone to disrupt and result in symptoms when compared with noncalcified plaques and carotid plaque calcification confers structural stability.[24] Fibrous cap inflammation and susceptibility to disruption are less likely to occur in calcified than in noncalcified plaques.[25]

Although QSM of carotid atherosclerosis was mentioned in an article,[26] histopathological correlation was not performed. To the best of our knowledge, this pilot study is the first to report QSM findings with histopathologic correlation. However, this study has several limitations. First, the small number of patients compromises the statistical power of the performed measurements. We therefore present these results as preliminary, suggestive rather than definitive findings. Second, we analyzed only the thickest plaque section of serial sections for one specimen, because it is difficult to evaluate the properties of small plaques due to pathological artifacts related to handling of the specimen and the low

spatial resolution of QSM at this time. Third, ROI of images were drawn manually with reference to pathological findings, and the susceptibility values may be biased. Forth, we did not use a water–fat separation method to remove the chemical shift by subcutaneous fat, which can affect the phase signal and QSM quantification. Fifth, imaging time of QSM was relatively long, and there was effect of motion artifacts caused by swallowing and vessel pulsation. They also could lead complex susceptibility values in some degree. Sixth, because there was no patient with fibrous plaque in our study, we could not discuss about fibrous component of plaque.

Conclusion

Intraplaque hemorrhages showed markedly high values on QSM. Lipid rich necrosis components showed various but significantly lower relative susceptibility values than intraplaque hemorrhages. QSM would be superior to conventional vessel wall images in distinct discrimination of intraplaque hemorrhage and lipid rich necrosis. Areas corresponding to calcification showed markedly low relative susceptibility values on QSM. QSM of carotid atherosclerotic plaque would provide a novel quantitative MRI contrast that enables reliable differentiation among intraplaque hemorrhage, lipid rich necrosis, and calcification.

Supplementary Information

(This supplementary is available online.)

Supplementary material 1
Case 2, plaque with hemorrhage, lipid rich necrosis, and calcification.
Red arrow and surrounded by red dot lines: hemorrhage.
Blue arrow and surrounded by blue dot lines: calcification.
Surrounded by green dot lines: lipid rich necrosis component.
White dot lines: lumen and outer layer of the artery.

Supplementary material 2
Case 3, plaque with lipid rich necrosis and calcification.

Supplementary material 3
Case 4, plaque with hemorrhage, lipid rich necrosis, and calcification.

Supplementary material 4
Case 5, plaque with hemorrhage and lipid rich necrosis.

Supplementary material 5
Case 6, plaque with lipid rich necrosis and calcification.

Supplementary material 6
Case 7, plaque with hemorrhage, lipid rich necrosis, and calcification.

Conflicts of Interest

Hiroshi Imai is an employee of Siemens Healthcare. The other authors declare that they have no conflicts of interest.

References

1. Chaturvedi S, Bruno A, Feasby T, et al. Carotid endarterectomy—an evidence-based review report of the Therapeutics and Technology Assessment Subcommittee of the American Academy of Neurology. Neurology 2005; 65:794–801.
2. Golledge J, Siew DA. Identifying the carotid 'high risk' plaque: is it still a riddle wrapped up in an enigma? Eur J Vasc Endovasc Surg 2008; 35:2–8.
3. Markus HS, King A, Shipley M, et al. Asymptomatic embolisation for prediction of stroke in the Asymptomatic Carotid Emboli Study (ACES): a prospective observational study. Lancet Neurol 2010; 9:663–671.
4. Underhill HR, Hatsukami TS, Fayad ZA, Fuster V, Yuan C. MRI of carotid atherosclerosis: clinical implications and future directions. Nat Rev Cardiol 2010; 7: 165–173.
5. Fryer JA, Myers PC, Appleberg M. Carotid intraplaque hemorrhage: the significance of neovascularity. J Vasc Surg 1987; 6:341–349.
6. Imparato AM, Riles TS, Gorstein F. The carotid bifurcation plaque: pathologic findings associated with cerebral ischemia. Stroke 1979; 10:238–245.
7. Howard DP, van Lammeren GW, Rothwell PM, et al. Symptomatic carotid atherosclerotic disease: correlations between plaque composition and ipsilateral stroke risk. Stroke 2015; 46:182–189.
8. Hosseini AA, Kandiyil N, Macsweeney ST, Altaf N, Auer DP. Carotid plaque hemorrhage on magnetic resonance imaging strongly predicts recurrent ischemia and stroke. Ann Neurol 2013; 73:774–784.
9. Sun J, Underhill HR, Hippe DS, Xue Y, Yuan C, Hatsukami TS. Sustained acceleration in carotid atherosclerotic plaque progression with intraplaque hemorrhage: a long-term time course study. JACC Cardiovasc Imaging 2012; 5:798–804.
10. Turc G, Oppenheim C, Naggara O, et al. Relationships between recent intraplaque hemorrhage and stroke risk factors in patients with carotid stenosis: the HIRISC study. Arterioscler Thromb Vasc Biol 2012; 32:492–499.
11. Cappendijk VC, Cleutjens KB, Heeneman S, et al. In vivo detection of hemorrhage in human atherosclerotic plaques with magnetic resonance imaging. J Magn Reson Imaging 2004; 20:105–110.
12. Cappendijk VC, Cleutjens KB, Kessels AG, et al. Assessment of human atherosclerotic carotid plaque components with multisequence MR imaging: initial experience. Radiology 2005; 234:487–492.
13. Moody AR, Murphy RE, Morgan PS, et al. Characterization of complicated carotid plaque with magnetic resonance direct thrombus imaging in patients with cerebral ischemia. Circulation 2003; 107:3047–3052.

14. Yuan C, Mitsumori LM, Ferguson MS, et al. In vivo accuracy of multispectral magnetic resonance imaging for identifying lipid-rich necrotic cores and intraplaque hemorrhage in advanced human carotid plaques. Circulation 2001; 104:2051–2056.
15. Chu B, Kampschulte A, Ferguson MS, et al. Hemorrhage in the atherosclerotic carotid plaque: a high-resolution MRI study. Stroke 2004; 35:1079–1084.
16. de Rochefort L, Liu T, Kressler B, et al. Quantitative susceptibility map reconstruction from MR phase data using bayesian regularization: validation and application to brain imaging. Magn Reson Med 2010; 63:194–206.
17. Schweser F, Sommer K, Deistung A, Reichenbach JR. Quantitative susceptibility mapping for investigating subtle susceptibility variations in the human brain. Neuroimage 2012; 62:2083–2100.
18. Wang Y, Liu T. Quantitative susceptibility mapping (QSM): decoding MRI data for a tissue magnetic biomarker. Magn Reson Med 2015; 73:82–101.
19. Yang Q, Liu J, Barnes SR, et al. Imaging the vessel wall in major peripheral arteries using susceptibility-weighted imaging. J Magn Reson Imaging 2009; 30:357–365.
20. Kerwin WS, Canton G. Advanced techniques for MRI of atherosclerotic plaque. Top Magn Reson Imaging 2009; 20:217–225.
21. Kolodgie FD, Gold HK, Burke AP, et al. Intraplaque hemorrhage and progression of coronary atheroma. N Engl J Med 2003; 349:2316–2325.
22. Yamada N, Higashi M, Otsubo R, et al. Association between signal hyperintensity on T1-weighted MR imaging of carotid plaques and ipsilateral ischemic events. AJNR Am J Neuroradiol 2007; 28:287–292.
23. Adams LC, Böker SM, Bender YY, et al. Detection of vessel wall calcifications in vertebral arteries using susceptibility weighted imaging. Neuroradiology 2017; 59:861–872.
24. Nandalur KR, Baskurt E, Hagspiel KD, Phillips CD, Kramer CM. Calcified carotid atherosclerotic plaque is associated less with ischemic symptoms than is noncalcified plaque on MDCT. AJR Am J Roentgenol 2005; 184:295–298.
25. Wahlgren CM, Zheng W, Shaalan W, Tang J, Bassiouny HS. Human carotid plaque calcification and vulnerability. Relationship between degree of plaque calcification, fibrous cap inflammatory gene expression and symptomatology. Cerebrovasc Dis 2009; 27: 193–200.
26. Liu S, Buch S, Chen Y, et al. Susceptibility-weighted imaging: current status and future directions. NMR Biomed 2017; 30:e3552.